



ORIGINAL ARTICLE

Dopamine Signaling Modulates the Stability and Integration of Intrinsic Brain Networks

Golia Shafiei ¹, Yashar Zeighami¹, Crystal A. Clark¹, Jennifer T. Coull^{2,3}, Atsuko Nagano-Saito^{1,4,5}, Marco Leyton^{1,5}, Alain Dagher¹ and Bratislav Mišić ¹

¹McConnell Brain Imaging Centre, Montréal Neurological Institute, McGill University, Montreal, QC, Canada, ²Laboratoire des Neurosciences Cognitives UMR 7291, Federation 3C, Aix-Marseille University, France, ³Centre National de la Recherche Scientifique (CNRS), Paris, France, ⁴Centre de Recherche, Institut Universitaire de Gériatrie de Montréal, Montréal, Canada and ⁵Department of Psychiatry, McGill University, Montréal, Canada

Address correspondence to Bratislav Mišić, McConnell Brain Imaging Centre, Montréal Neurological Institute, McGill University, 3801 Rue University, Montréal QC, H3A 2B4 Canada. Email: bratislav.misic@mcgill.ca  orcid.org/0000-0003-0307-2862

Abstract

Dopaminergic projections are hypothesized to stabilize neural signaling and neural representations, but how they shape regional information processing and large-scale network interactions remains unclear. Here we investigated effects of lowered dopamine levels on within-region temporal signal variability (measured by sample entropy) and between-region functional connectivity (measured by pairwise temporal correlations) in the healthy brain at rest. The acute phenylalanine and tyrosine depletion (APTD) method was used to decrease dopamine synthesis in 51 healthy participants who underwent resting-state functional MRI (fMRI) scanning. Functional connectivity and regional signal variability were estimated for each participant. Multivariate partial least squares (PLS) analysis was used to statistically assess changes in signal variability following APTD as compared with the balanced control treatment. The analysis captured a pattern of increased regional signal variability following dopamine depletion. Changes in hemodynamic signal variability were concomitant with changes in functional connectivity, such that nodes with greatest increase in signal variability following dopamine depletion also experienced greatest decrease in functional connectivity. Our results suggest that dopamine may act to stabilize neural signaling, particularly in networks related to motor function and orienting attention towards behaviorally-relevant stimuli. Moreover, dopamine-dependent signal variability is critically associated with functional embedding of individual areas in large-scale networks.

Key words: connectome, dopamine depletion, functional connectivity, neural dynamics, signal variability

Introduction

The brain is a complex network of interacting neuronal populations that collectively support perception, cognition, and action. Transient episodes of synchrony establish brief windows for communication among remote neuronal populations,

manifesting as patterns of functional connectivity and large-scale resting state networks (Damoiseaux et al. 2006; Power et al. 2011; Yeo et al. 2011). Thus, regional neural activity reflects computations that result from network interactions, but also drives those interactions (Deco et al. 2010; Avena-

Koenigsberger et al. 2018). Greater connectivity may promote greater signal exchange, leading to variable dynamics (Rubinov et al. 2009; Mišić et al. 2011); alternatively, densely interconnected regions may be more likely to synchronize, rendering their dynamics less variable and more stable (Gollo et al. 2015). How the balance between local dynamics and global functional interactions (connectivity) is modulated remains a fundamental question in systems neuroscience.

Dopamine is thought to stabilize neuronal signaling by modulating synaptic activity and signal gain (Seamans and Yang 2004). Dopamine, acting in cortex or striatum, could regulate cortical representations by facilitating or suppressing neural signaling. These effects may also play a role in reinforcement learning, based on the theory of dopaminergic reward prediction error signaling (Schultz 2002). In humans, transient decreases in dopamine synthesis (which we term “dopamine depletion”) have been shown to disrupt multiple aspects of perception, motor control, and executive function (Nagano-Saito et al. 2008, 2012; Coull et al. 2012; Ramdani et al. 2015), consistent with a role in the regulation of sustained cortical activity (Seamans and Yang 2004). Similar effects have also been demonstrated in various animal models including rodents and monkeys (Seamans and Robbins 2010). Furthermore, death of dopamine neurons in Parkinson’s disease (PD) leads to unstable and increasingly variable motor output (McAuley 2003; Björklund and Dunnett 2007). Thus, by stabilizing neuronal signaling, dopamine may influence the stability of regional activity and its potential for functional interactions at a network level.

Here we use resting-state functional magnetic resonance imaging (fMRI) to investigate the effects of dopamine depletion on within region signal variability and intrinsic brain networks in healthy brain at rest. We applied acute phenylalanine and tyrosine depletion (APTD) to transiently decrease dopamine levels in healthy participants (Palmour et al. 1998; McTavish, Cowen et al. 1999; Leyton et al. 2000, 2004; Montgomery et al. 2003; Carbonell et al. 2014). We hypothesized that dopamine depletion would destabilize regional hemodynamic activity, manifesting as increased signal variability. We further hypothesized that regions with increased signal variability may be less likely to interact with other regions, resulting in decreased functional connectivity defined by temporal statistical association of fMRI time series.

Materials and Methods

Participants

Altogether, $n = 51$ healthy young individuals (right-handed, 23.6 ± 5.9 years old, 32 male/19 female) participated in 3 separate dopamine precursor depletion studies (two published (Coull et al. 2012; Nagano-Saito et al. 2012) and one unpublished study). The protocol, acquisition site, scanner and sequence were identical across the 3 studies. Participants with a history of drug abuse, neurological, or psychiatric disorder were excluded. Informed consent was obtained from all participants.

Dopamine Depletion

The APTD technique (Palmour et al. 1998; McTavish, McPherson et al. 1999; Leyton et al. 2000) was used to reduce dopamine synthesis in healthy participants, following the procedure described previously (Coull et al. 2012; Nagano-Saito et al. 2012). In short, each participant was tested twice on 2 separate days, once following administration of a nutritionally balanced

amino acid mixture (BAL) and once following acute phenylalanine/tyrosine depletion (APTD), in a randomized, double-blind manner, such that neither the participants nor the experiment conductors had any information regarding the label of the condition (BAL vs. APTD) being tested on each day. It should be noted that although APTD leads to depletion of dopamine precursors and only reduces the dopamine synthesis and availability, the term “dopamine depletion” is used throughout this manuscript to refer to “dopamine precursor depletion” and APTD. Although APTD might also theoretically decrease norepinephrine synthesis, several reports have shown that the release of norepinephrine is not affected under resting state conditions (McTavish, Cowen et al. 1999; Le Masurier et al. 2014).

Data Acquisition and Preprocessing

T1-weighted, three-dimensional structural MRIs were acquired for anatomical localization (1-mm³ voxel size), as well as two resting-state echoplanar T2*-weighted images with blood oxygenation level-dependent (BOLD) contrast (3.5-mm isotropic voxels, TE 30 ms, TR 2 s, flip angle 90°) from all participants using a Siemens MAGNETOM Trio 3 T MRI system at the Montréal Neurological Institute (MNI) in Montréal, Canada. Each participant was scanned for 5 min (150 volumes) with eyes open, on 2 separate days, once following administration of a nutritionally balanced amino acid mixture (BAL) and once following acute phenylalanine/tyrosine depletion (APTD). The resting state fMRI data was preprocessed through the following steps: slice timing correction, rigid body motion correction, removal of slow temporal drift using a high-pass filter with 0.01 Hz cut-off, physiological noise correction. Head motion parameters were estimated by spatially re-aligning individual time points with the median volume, which was then aligned with the anatomical T1 image of the individual. Further motion correction was done by scrubbing (Power et al. 2012): time points with excessive in-scanner motion (>0.5 mm framewise displacement) were identified and removed from time series, along with the two volumes before and two volumes after. All preprocessing steps were performed using the Neuroimaging Analysis Kit (NIAK) (Bellec et al. 2010, 2012).

Anatomical MRI data was parceled into 83 cortical and sub-cortical areas using the Desikan-Killiany atlas (Desikan et al. 2006), and then further subdivided into 129, 234, 463, and 1015 approximately equally sized parcels following the procedure described by Cammoun and colleagues (2012). The Desikan-Killiany atlas is a commonly-used, anatomical (as opposed to functional), automated labeling system, where nodes are delineated according to anatomical landmarks. It has been shown that the Desikan-Killiany atlas is comparably reliable to manual parcellations of human cortex (Desikan et al. 2006). The atlas exists at 5 progressively coarser resolutions (the so-called “Lausanne” parcellation; Cammoun et al. 2012), allowing us to verify the experimental effects on various spatial scales. The parcellations were used to extract BOLD time series from functional MRI data. The time series of each parcel were estimated as the mean of all voxels in that parcel. All analyses were repeated at each resolution to ensure that none of the conclusions were idiosyncratic to a particular spatial scale.

Sample Entropy

Sample entropy (SE) analysis was used to estimate within-region signal variability (Richman and Moorman 2000). The

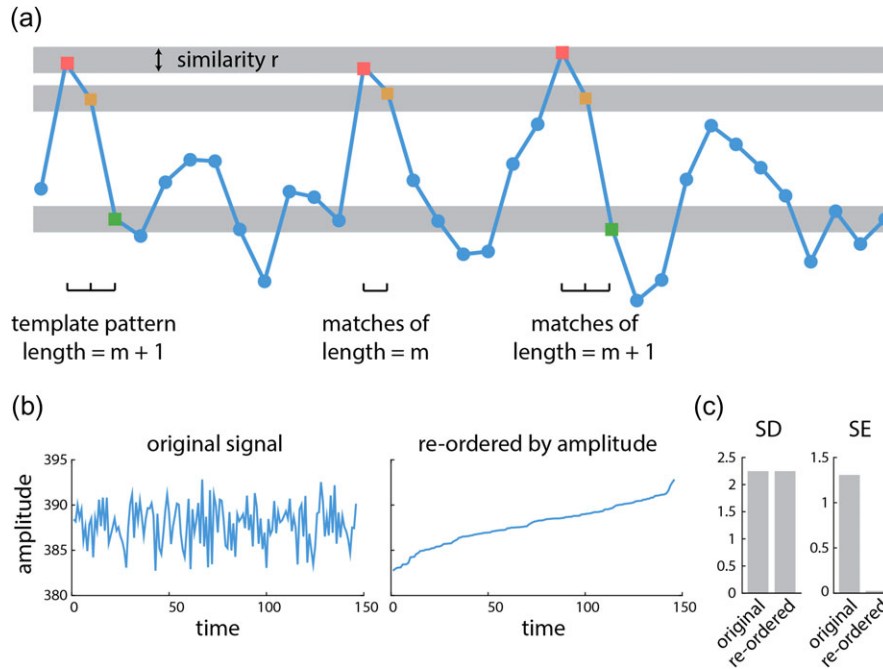


Figure 1. Sample entropy of a time series | (a) An example of a BOLD signal is shown, where the x-axis is time and the y-axis is the amplitude. Signal variability is calculated using sample entropy analysis. Sample entropy (SE) measures the conditional probability that any two sequences of data points with length $m + 1$ will be similar to one another under the condition that they were similar for the first m points. The similarity criterion r represents the tolerance of algorithm to accept matches in the time series. (b) An example of a BOLD signal in its original form (left). The same signal, with the time points reordered by amplitude (right). (c) Standard deviation of the signal is the same for both the original and reordered signal; however, sample entropy of the reordered signal drastically decreases compared with sample entropy of the original signal.

algorithm quantifies the conditional probability that any two sequences of time points with length of $m + 1$ will be similar to each other, given that the first m points of these sequences were similar (Fig. 1). SE is defined as the natural logarithm of this quantity, such that large values are assigned to unpredictable signals, and small values to predictable signals. The algorithm is subject to 2 parameters: the pattern length (m), which determines the segment length used to detect repeating patterns, and the similarity criterion (r), which is the tolerance for accepting matches in the time series. The sample entropy of a time series with length N is estimated as

$$SE(m, r, N) = \ln \frac{\sum_{i=1}^{N-m} n_i^m}{\sum_{i=1}^{N-m} n_i^{m+1}}$$

where n_i^m is the number of m -length segment of time series (e.g., segment j with length m) that are similar to the m -length segment i within the similarity criterion, excluding self-matches ($i \neq j$; i.e., the algorithm does not compare patterns with themselves) (Costa et al. 2005). The sample entropy of a time series corresponds to “scale 1” of the well-known multi-scale entropy analysis procedure (Costa et al. 2005).

Following the optimization proposed by Small and Tse (2004), we set $m = 2$ as the pattern length. We set the similarity criterion to $r = 0.5$ times the standard deviation (SD) of the time series following the method proposed by Richman and Moorman (2000). Although these values of m and r have been used extensively in previous reports (McIntosh et al. 2008; Beharelle et al. 2012; Heisz et al. 2012; Mišić et al. 2016), we sought to ensure that the reported results were robust across multiple choices of m and r . We therefore re-calculated SE using different values for m and r and re-ran the PLS analysis described below (see Statistical assessment). Figure S2 shows

the correlation between new bootstrap ratios (i.e., changes in signal variability) with bootstrap ratios that were originally estimated by setting $m = 2$ and $r = 0.5 \times SD$. The correlations were generally greater than 0.7 across a range of similarity criteria r , and greater than 0.3 across a range of pattern lengths m , suggesting that the results were relatively insensitive to choice of parameters.

We operationalized signal variability using SE rather than other popular measures, such as standard deviation (SD). The primary reason for this choice is that SE is sensitive to temporal dependencies in the signal, while variance-based measures, such as SD, are not. This distinction is illustrated in Figure 1b and c. Figure 1b (left) shows a typical BOLD signal from the present study (a randomly selected condition, participant and node). Figure 1b (right) shows the same signal, but with the time points reordered by amplitude. The sample entropy and standard deviation of the original and reordered signals were then measured (Fig. 1c). Sample entropy is sensitive to this change, because the reordered signal monotonically increases and is trivially predictable. Critically, standard deviation is blind to this change; although the temporal complexity of the signal has been profoundly altered by reordering, standard deviation measures only the dispersion of points and cannot detect any temporal change (Fig. 1c).

Statistical Assessment

We used partial least squares (PLS) analysis to investigate within-participant changes in regional signal variability following the BAL versus APTD conditions. PLS analysis is a multivariate statistical technique that is used to analyze two “blocks” or sets of variables (McIntosh and Lobaugh 2004; McIntosh and Mišić 2013). In neuroimaging studies, one set may represent

neural activity, while the other may represent behavior or experimental design (e.g., condition and/or group assignments). PLS analysis seeks to relate these two data blocks by constructing linear combinations of the original variables such that the new latent variables have maximum covariance (Krishnan et al. 2011).

In the present report, one block (\mathbf{X}) corresponded to regional signal variability for each participant estimated by sample entropy of BOLD time series following BAL versus APTD conditions. The rows of matrix \mathbf{X} correspond to observations (participants nested within conditions) and the columns correspond to variables (regional signal variability). For p participants, c conditions, and v variables, matrix \mathbf{X} will have $p \times c$ rows and v columns. Within-condition means are computed for each column and centered to give the matrix \mathbf{M} . Singular value decomposition (SVD) is applied to \mathbf{M}

$$\mathbf{USV} = \mathbf{M}$$

resulting in a set of orthonormal left singular vectors, \mathbf{U} , and right singular vectors, \mathbf{V} , and a diagonal matrix of singular values, \mathbf{S} . The number of latent variables is equal to the rank of the mean-centered matrix (here c), so \mathbf{U} will have c columns and v rows, and \mathbf{V} and \mathbf{S} will both have c columns and c rows.

The decomposition results in a set of latent variables that are composed of columns of singular vectors, \mathbf{U} and \mathbf{V} , and a set of singular values from the diagonal matrix of \mathbf{S} . In the present study, the v elements of column vectors of \mathbf{U} are the weights of original brain activity variables (i.e., signal variability) that contribute to the latent variable and demonstrate a pattern of changes in signal variability following dopamine depletion. The c elements of column vectors of \mathbf{V} are the weights of experimental design variables that contribute to the same latent variable and are interpreted as a contrast between experimental conditions. The latent variables are mutually orthogonal and express the shared information between the two data blocks with maximum covariance. This covariance is reflected in the singular values from the diagonal elements of matrix \mathbf{S} that are associated with each given latent variable.

We assessed the statistical significance of each latent variable using permutation tests (Edgington and Onghena 2007). During each permutation, condition labels for each participant are randomized by reordering the rows of matrix \mathbf{X} . The new permuted data matrices were then mean-centered and subjected to SVD as before. The procedure was repeated 10 000 times to generate a distribution of singular values under the null hypothesis that there is no relationship between neural activity and study design. A p -value was estimated for each latent variable as the proportion of permuted singular values greater than or equal to the original singular value.

We assessed the reliability of singular vector weights using bootstrap resampling. Here, the rows of data matrix \mathbf{X} were randomly resampled with replacement while keeping the original condition assignments. Mean-centering and SVD were then applied to the resampled data matrices as before. The results were used to build a sampling distribution for each weight in the singular vectors \mathbf{U} and \mathbf{V} . A “bootstrap ratio” was then calculated for each original variable (i.e., for each node) as the ratio of the singular vector weight to its bootstrap-estimated standard error. Bootstrap ratios are designed to be large for variables that have a large weight (i.e., large contribution) as well as a small standard error (i.e., are stable). Bootstrap ratios are equivalent to z -scores if the bootstrap distribution is approximately unit normal (Efron and Tibshirani 1986). In this

case, 95% and 99% confidence intervals correspond to bootstrap ratios of ± 1.96 and ± 2.58 , respectively.

PLS was chosen as the primary analytic method (instead of univariate statistical techniques) because we sought to identify patterns of nodes whose signal variability collectively changes due to dopamine depletion. However, the results of PLS analysis were nearly identical with the results obtained by a more conventional univariate paired t -test (correlation between t -values and bootstrap ratios; $r \approx 1$).

Community Detection

Functional networks were partitioned into communities or intrinsic networks using the assignment derived in Mišić et al. (2015a), which we describe below. As we show in the Results section, the main conclusions also hold for the partitions reported by Yeo and colleagues (Yeo et al. 2011) and Power and colleagues (Power et al. 2011).

A Louvain-like greedy algorithm was used to identify a community assignment that maximized the quality function, Q (Newman and Girvan 2004; Rubinov and Sporns 2011)

$$Q(\gamma) = \frac{1}{m^+} \sum_{ij} (W_{ij}^+ - \gamma p_{ij}^+) \delta(\sigma_i, \sigma_j) - \frac{1}{m^+ + m^-} \sum_{ij} (W_{ij}^- - \gamma p_{ij}^-) \delta(\sigma_i, \sigma_j)$$

where W_{ij}^+ and W_{ij}^- are the functional connectivity (correlation) matrices that contain only positive and only negative coefficients of correlation, respectively. p_{ij}^+ is the expected density of only positive or only negative connectivity matrices according to the configuration null model and is given as $p_{ij}^+ = (s_i^+ s_j^+) / 2m^+$. $m^+ = \sum_{i,j>i} W_{ij}^+$ is the total weight of all positive or negative connections of W_{ij}^+ (note that the summation is taken over $i, j > i$ to ensure that each connection is only counted once). The total weights of positive or negative connections of i and j are given by $s_i^+ = \sum_j W_{ij}^+$ and $s_j^+ = \sum_i W_{ij}^+$, respectively. The resolution parameter γ scales the importance of the null model and effectively controls the size of the detected communities: larger communities are more likely to be detected when $\gamma < 1$ and smaller communities (with fewer nodes in each community) are more likely to be detected when $\gamma > 1$. Furthermore, σ_i defines the community assignment of node i . The Kronecker function $\delta(\sigma_i, \sigma_j)$ is equal to 1 if $\sigma_i = \sigma_j$ and is equal to zero otherwise ($\sigma_i \neq \sigma_j$), ensuring that only within-community connections contribute to Q .

Multiple resolutions γ were assessed, from 0.5 to 10 in steps of 0.1. The Louvain algorithm was repeated 250 times for each γ value (Blondel et al. 2008). The resolution $\gamma = 1.5$ was chosen based on the similarity measures (Rand index) of pairs of partitions for each γ value, such that the similarity measures of a more stable set of partitions for a given γ value would have a larger mean and smaller standard deviation compared with similarity measures at other γ values (i.e., larger z -score of similarity measure) (Traud et al. 2011). Finally, a consensus partition was found from the 250 partitions at $\gamma = 1.5$ following the method described in Bassett et al. (2013). Eight communities or networks were detected, including visual (VIS), temporal (TEM), default mode (DMN), dorsal attention (DA), ventral attention (VA), somatomotor (SM), and salience (SAL) (Mišić et al. 2015a). The subcortical areas (SUB) were added to the list as a separate network based on the anatomical Desikan-Killiany parcellation.

Cohesion and Integration

Connectivity between and within modules was assessed as the participation coefficient and within-module degree z-score (Guimerà and Amaral 2005), using Brain Connectivity Toolbox (BCT) (Rubinov and Sporns 2010). The participation coefficient quantifies how evenly distributed a node's connections are to all modules. Values close to 1 indicate that a node is connected to many communities, while values close to 0 indicate that a node is connected to few communities. The participation coefficient of node i , P_i , is given by

$$P_i = 1 - \sum_{m \in M} \left(\frac{k_i(m)}{k_i} \right)^2$$

where m is a module from a set of modules M , k_i is the weighted degree (i.e., connection strength) of node i , and $k_i(m)$ is the number of connections between node i and all other nodes in module m (Guimerà and Amaral 2005; Rubinov and Sporns 2010). To find participation coefficients of resting state networks, we first found the average participation coefficient of each node across all participants and then compared the participation coefficients of the nodes that belong to the same module following the BAL versus APTD conditions.

The within-module degree is estimated as the weighted degree (i.e., strength) of the connections that node i makes to other nodes within the same module. The measure is then z-scored, expressing a node's weighted degree in terms of standard deviations above or below the mean degree of the nodes in the given module (Z_i). A positive within-module degree z-score indicates that a node is highly connected to other nodes within the same module, while a negative within-module z-score indicates a node participates in less than average connections within its own module. We estimated the within-module degree z-score of each node for each participant and then calculated the average Z_i over all participants. Finally, we compared the within-module degree z-scores of the nodes of a given module following the BAL and APTD conditions.

Results

Task-free, eyes-open resting-state fMRI was recorded in $n = 51$ healthy young participants on 2 separate days, once following

administration of a nutritionally balanced amino acid mixture (BAL) and once following acute phenylalanine/tyrosine depletion (APTD). Anatomical MRI data were parceled into 5 progressively finer resolutions, comprising 83, 129, 234, 463, and 1015 nodes (Cammoun et al. 2012), which were used for extraction of blood-oxygen-level dependent (BOLD) time series. We investigated how dopamine depletion affects (a) local, region-level hemodynamic activity, (b) global, between-region temporal statistical association of BOLD time series (termed as “functional connectivity”), and (c) the relationship between the two.

Dopamine Depletion Increases Signal Variability

We estimated within region signal variability using sample entropy (SE), a measure of the unpredictability of a time series (Richman and Moorman 2000). Briefly, the SE algorithm quantifies the conditional probability that any two sequences of $m + 1$ time points will be similar to each other given that the first m points were similar (Fig. 1). We then used multivariate partial least squares (PLS) analysis to statistically assess within-participant changes in signal variability at each brain region following administration of the BAL versus APTD mixtures (McIntosh and Mišić 2013). PLS results in a set of latent variables (LV), that are weighted combinations of experimental design (i.e., a contrast) and signal variability patterns that optimally covary with each other. The analysis revealed a single statistically significant latent variable (permuted $p = 0.014$ for the finest parcellation resolution with 1015 nodes), showing broadly increased signal variability following dopamine depletion (Fig. 2). Bootstrap resampling was used to estimate the reliability with which individual nodes contribute to the overall multivariate pattern. Specifically, the weight or loading associated with each node was divided by its bootstrap-estimated standard error, yielding a measure (“bootstrap ratio”) that is high for nodes with large weights (i.e., large contributions) and small standard errors (i.e., are stable) (McIntosh and Lobaugh 2004). Note that bootstrap ratios may be interpreted as z-scores if the sampling distribution is approximately unit normal (Efron and Tibshirani 1986). Positive bootstrap ratios indicate an increase in signal variability, while negative bootstrap ratios indicate decreased variability. Figure 2c depicts a brain projection of this statistical pattern, showing that the greatest

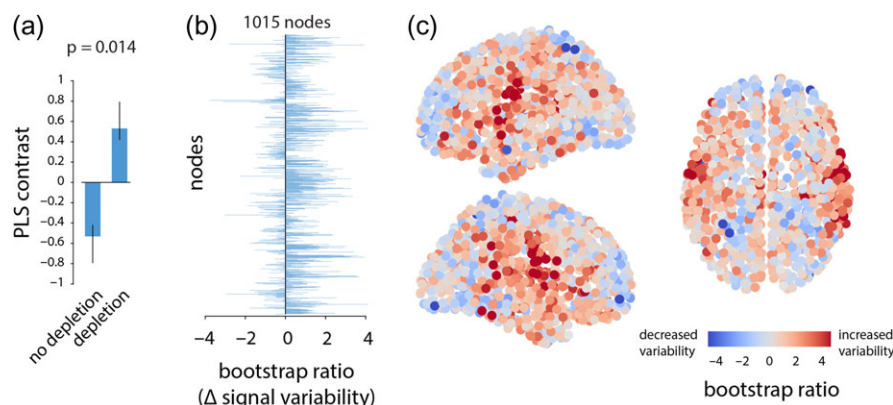


Figure 2. Dopamine depletion increases signal variability | (a) PLS analysis identified a significant contrast between patterns of signal variability in depletion (APTD) versus non-depletion (BAL) conditions (permuted $P = 0.014$). (b) The change in signal variability of each node is given by a bootstrap ratio for that node: such that a positive bootstrap ratio shows increase in signal variability of the node following dopamine depletion, while a negative bootstrap ratio shows the opposite. Bootstrap ratios are depicted at the finest resolution (1015 nodes), showing that dopamine depletion increases signal variability at most nodes. (c) Bootstrap ratios are shown in 3D space sagittally and axially. Corresponding results are shown for all resolutions in Figure S1.

increase in signal variability was observed in somatomotor cortex. This effect (increased regional hemodynamic variability following depletion) and the spatial pattern were consistent across all 5 spatial resolutions (Fig. S1).

Increased Signal Variability in Somatomotor and Saliency Networks

We next investigated the effect of APTD on resting state networks (Power et al. 2011; Yeo et al. 2011). Figure 3a depicts the nodes displaying the greatest increase in signal variability following dopamine depletion in descending order and color-coded by resting state network membership (Mišić et al. 2015a). The most affected nodes appear to belong primarily to the somatomotor (yellow) and saliency (green) networks suggesting that the signal variability may selectively affect certain large-scale networks.

To directly investigate the network-selectivity of dopamine depletion, we first estimated the mean change in signal variability across all nodes in a given network, using PLS-derived bootstrap ratios for the finest resolution (1015 nodes). To determine which network-level changes were statistically significant and not due to differences in network size, spatial contiguity or lateralization, we used a label permuting procedure. Network labels were randomly permuted within each hemisphere (preserving the number of nodes assigned to each network) and network means were recomputed 10000 times, generating a distribution under the null hypothesis that network assignment does not influence the overall change in signal variability. A p -value was estimated for each network as the proportion of cases when the mean for the permuted network assignment exceeded the mean for the original empirical network assignment. Figure 3b,c shows that changes in signal variability were observed for all intrinsic networks, but that increased variability was greatest and statistically significant for the

somatomotor and saliency networks ($p < 10^{-4}$, FDR corrected (Benjamini and Hochberg 1995)).

To ensure that these results are independent of how intrinsic networks are defined, we repeated the procedure using partitions reported by Yeo and colleagues (Yeo et al. 2011) and by Power and colleagues (Power et al. 2011) (Fig. S3). The results were consistent across the 3 partitions, indicating significant increased signal variability in somatomotor and ventral attention networks among Yeo networks (note that the “ventral attention network” overlaps with the “saliency network” shown in Fig. 3), and in somatosensory and auditory networks among Power networks. No significant decrease in signal variability was observed in any other intrinsic networks, regardless of which network assignments were used.

Increased Signal Variability Correlates With Decreased Functional Connectivity

Given that changes in signal variability were highly network dependent, we next investigated whether increased signal variability is related to patterns of functional connectivity. Functional connectivity was estimated as a zero-lag Pearson correlation coefficient between regional time series for each participant in each condition. To relate patterns of signal variability with functional connectivity, we estimated a group-average functional connectivity matrix by calculating the mean connectivity of each pair of brain regions across all participants. We then estimated the mean connectivity (i.e., strength of the functional correlations) for each brain region.

We observed a weak relationship between increased signal variability and decreased functional connectivity, such that nodes with the greatest increase in signal variability following dopamine depletion also experienced the greatest decrease in functional connectivity ($r = -0.23$, $R^2 = 0.053$, $p = 1.04 \times 10^{-13}$; Fig. 4a). Although statistically significant, effect was small,

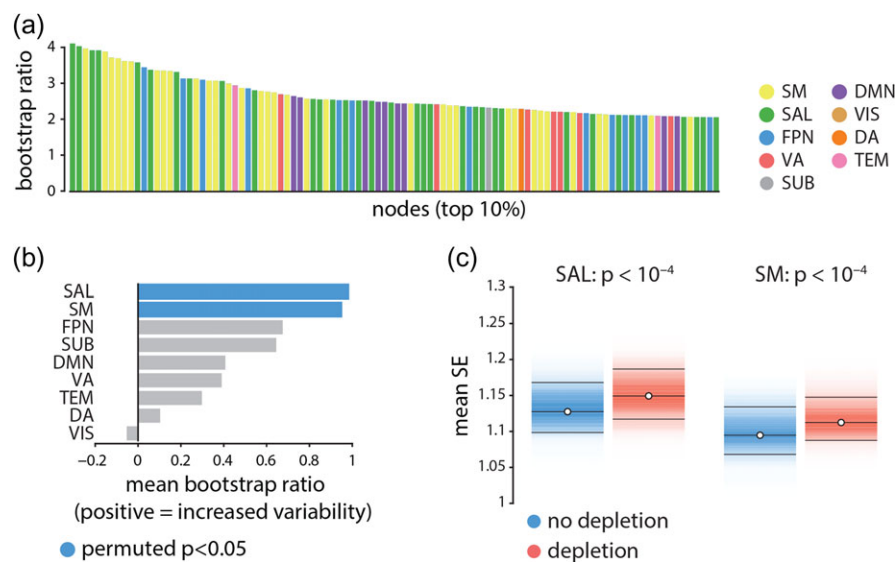


Figure 3. Node- and network-level effects of dopamine depletion | (a) The top 10% of the nodes (i.e., top 100 nodes) that had the largest increase in signal variability (largest bootstrap ratios) following dopamine depletion. Each bar shows the magnitude of bootstrap ratio of a node and is colored based on the community assignment of that node (Mišić et al. 2015a). Somatomotor (yellow) and saliency (green) networks appear over-represented compared with other networks. (b) The mean change in signal variability is calculated for each network and assessed by permutation tests (10000 repetitions). Signal variability increases most in the saliency and somatomotor networks following dopamine depletion, and these are the only two networks where this effect is statistically significant. (c) Changes in mean signal variability are depicted for somatomotor and saliency networks (significance obtained by permutation tests; FDR corrected (Benjamini and Hochberg 1995)). SM = somatomotor, SAL = saliency, FPN = fronto-parietal, VA = ventral attention, SUB = subcortical areas, DMN = default mode, VIS = visual, DA = dorsal attention, TEM = temporal.

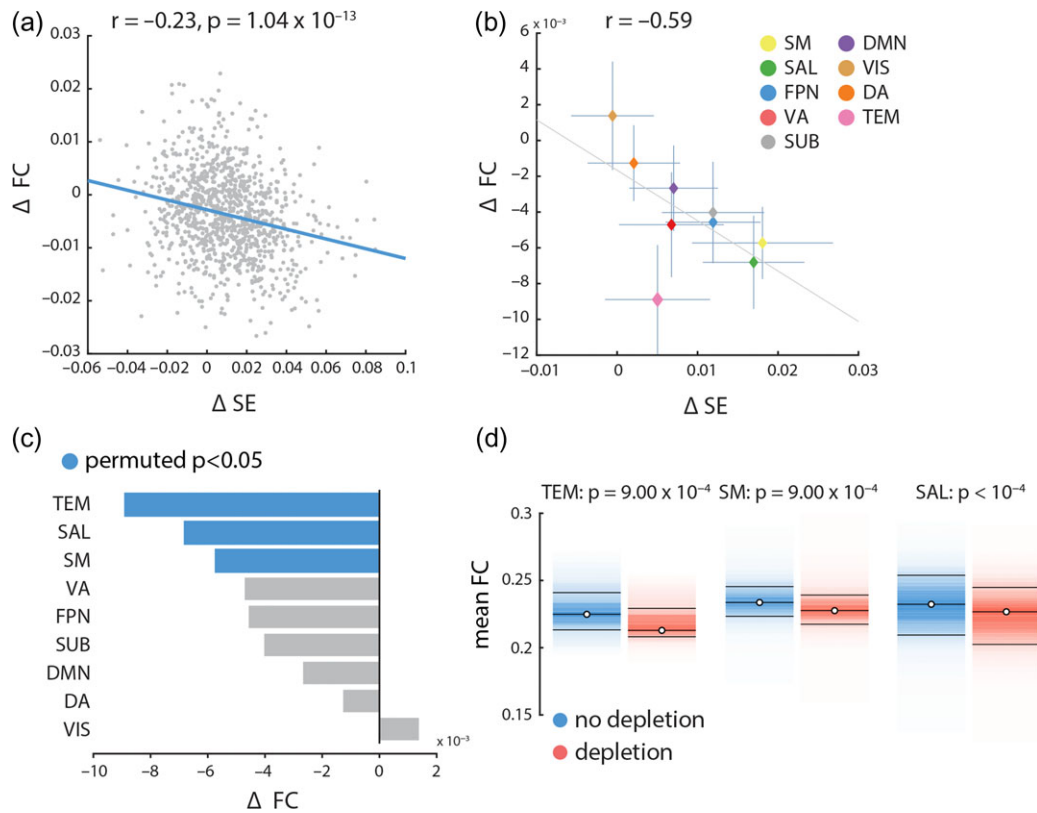


Figure 4. Relating signal variability and functional connectivity | (a) Mean changes in functional connectivity following dopamine depletion were estimated across all nodes and correlated with changes in within-region signal variability. Changes in functional connectivity are related to changes in signal variability, such that the larger the increase in signal variability, the larger the decrease in functional connectivity. (b) Mean changes in functional connectivity for intrinsic networks are correlated with mean changes in local signal variability in those networks. There is a clear anti-correlation between the two, consistent with the result in part (a). (c) The mean changes in functional connectivity was calculated for each network and assessed by permutation tests (10 000 repetitions). Mean connectivity significantly decreases in temporal, salience and somatomotor networks. Somatomotor and salience networks also experience significant increase in local variability (Fig. 3). (d) Mean functional connectivity in depletion (APTD) versus non-depletion (BAL) conditions, shown for nodes belonging to the temporal (TEM), somatomotor (SM) and salience (SAL) networks. Functional connectivity decreases in all instances (permutation test; FDR corrected).

suggesting that the relationship was not sustained over the bulk of data points (nodes), but that it may have been driven by a subset of nodes instead.

To investigate this possibility, we assessed mean dopamine-dependent changes in functional connectivity in each of the intrinsic networks separately and correlated the network specific changes in functional correlation with the network specific changes in signal variability. Note that these analyses did not estimate subject error, but modeled group-averaged effects. Although there is a significant negative correlation between changes in functional connectivity and signal variability in more than half of the participants (29 out of 51), positive or no correlation was observed in others (7 and 15 out of 51 participants, respectively). In other words, the group-level effect is consistent with individual-level effects in the majority of participants. This result is broadly consistent with previous studies of group- versus individual-level effects of dopaminergic manipulations (Garrett et al. 2015; Alavash et al. 2018) and indicates that further investigation is required to assess the effects of dopamine depletion at the individual participant level. The results provided in the present work mainly address the group-level effects of dopamine depletion.

Thus, on the group-level, we observed an anti-correlation between the two measures such that the networks with greatest increase in hemodynamic signal variability also experience the great decrease in functional correlations ($r = -0.59$; Fig. 4b).

Changes in functional connectivity were statistically assessed using the same label permuting procedure outlined above (randomly permuting the network label of all nodes and re-computing network means, with 10 000 repetitions). Mean functional connectivity significantly decreased in 3 intrinsic networks: temporal, salience, and somatomotor networks connectivity ($p = 9.0 \times 10^{-4}$, $p < 10^{-4}$ and $p = 9.0 \times 10^{-4}$ respectively; FDR corrected; Fig. 4c,d). Critically, the salience and somatomotor networks also experienced the greatest increase in signal variability after APTD (Fig. 3), suggesting that changes in signal variability and functional connectivity may be related. Overall, these results suggest that the effects of dopamine depletion are stronger in specific large-scale systems, and that changes in local dynamics are related to global functional interactions.

Selective Disconnection of Intrinsic Networks

Dopamine-related increases in signal variability appear to be concomitant with decreased functional connectivity and localized to specific intrinsic networks. However, it is unclear whether decreased connectivity in the somatomotor and salience networks is driven by weakened within-network or between-network connections, or both. To address this question, we calculated the participation coefficient and within-module degree z-score of every node (Guimerà and Amaral

2005). The participation coefficient quantifies the diversity of a node's connectivity profile. A participation coefficient with a value close to 1 indicates that a node's connections are evenly distributed across communities, while a value close to 0 indicates that most of the node's connections are within its own community. The within-module degree z-score of a node is a normalized measure of the strength of connections a node makes within its own community.

Figure 5 shows that the participation coefficient significantly decreases in somatomotor and salience networks following dopamine depletion ($p = 10^{-4}$ and $p = 2.4 \times 10^{-3}$, respectively, assessed by label permuting (see above); FDR corrected), while the within-module degree z-score does not ($p = 0.5$). In other words, dopamine depletion selectively reduced functional interactions between these networks and the rest of the brain (participation coefficient; Fig. 5a), but did not affect within-network cohesion (within-module degree z-score; Fig. 5b). Overall, these results suggest that dopamine depletion effectively segregates these intrinsic networks from the rest of the brain, but does not affect their internal cohesion. Note that the two networks with significantly decreased participation coefficient are also the ones with greatest increases in signal variability. We also investigated average changes in participation coefficient and within-module degree z-score in other intrinsic networks, where we did not observe any significant changes in either of the two measures.

No Systematic Effect of Study

The data used in this study were consolidated from 3 different experiments (2 published; Coull et al. 2012; Nagano-Saito et al. 2012 and one unpublished study), so it is possible that the observed effects were idiosyncratic to one or two of the

constituent datasets and do not necessarily generalize across all 3 studies. To investigate this possibility, we used a multi-way ANOVA to assess differences between studies: participant-specific scores were calculated for the signal variability pattern and the 3 studies were treated as separate groups. The analysis did not reveal any significant difference among the 3 studies ($F(2, 45) = 1.7, p = 0.19$), nor any condition by study interaction ($F(2, 45) = 0.68, p = 0.51$). There was a significant condition difference, with greater scores in the depletion versus non-depletion condition ($F(1, 45) = 131.06, p \approx 0$), but this is expected given that the scores were derived by PLS to maximize this condition difference.

Comparing Sample Entropy and Standard Deviation

A popular alternative measure of signal variability is the simple standard deviation (SD). Although we opted to use SE over SD because the latter is not sensitive to temporal dependencies in the signal (see Fig. 1), for completeness we directly compared the effects of depletion using the two measures. A priori, we expect the two measures to be anti-correlated, because sample entropy estimation explicitly incorporates the SD of a given signal to define the similarity criterion r (the tolerance of the algorithm to accept matches in the time series). For a deeper discussion of this practice, including potential limitations, see Grandy et al. (2016). In other words, the similarity criterion for the sample entropy algorithm will be greater for a signal with a greater SD. Consequently, the sample entropy algorithm is more likely to identify matches in signals with a larger SD, resulting in a lower sample entropy value. To demonstrate this claim, we correlated the SD and sample entropy of regional time series for both APTD (depletion) and BAL (no depletion) conditions, as well as the changes in each measure following

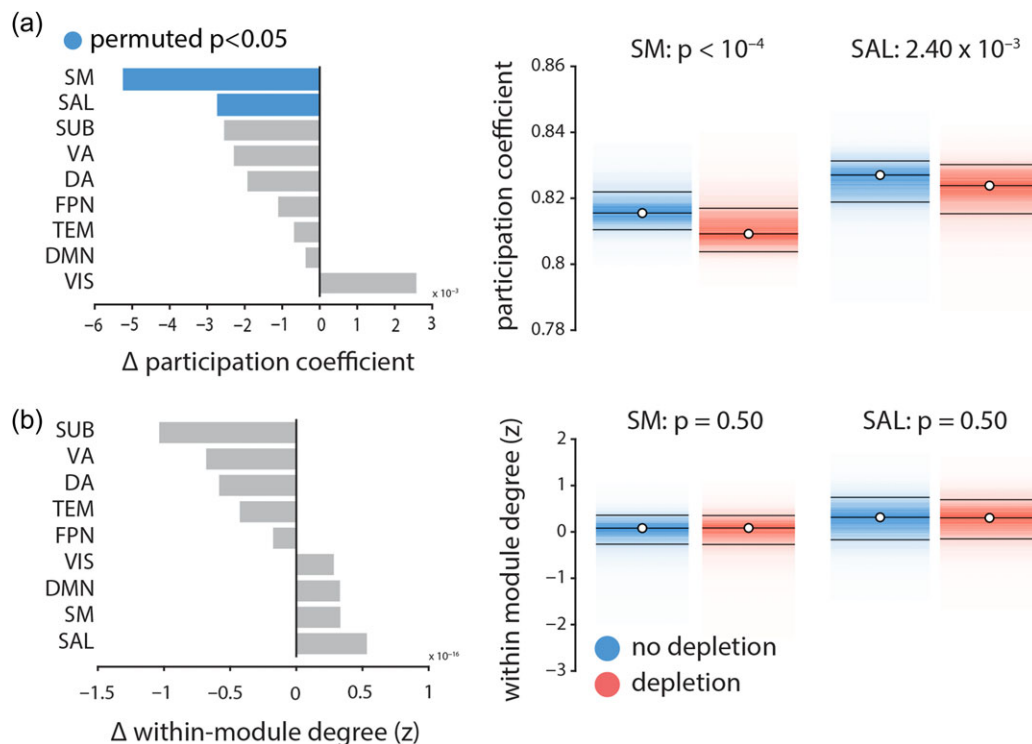


Figure 5. The effects of dopamine depletion on cohesion and integration of specific intrinsic networks | (a) Mean participation coefficient, indexing the diversity of inter-network connectivity, significantly decreases in somatomotor (SM) and salience (SAL) networks after dopamine depletion (using 10 000 permutation tests; FDR corrected). (b) Within-module degree z-score, indexing within-network connectivity, remains unaffected.

dopamine depletion. The results are shown in Figure S4, confirming the anti-correlation between sample entropy and SD of a given signal at a brain region in the (a) no depletion condition, (b) depletion condition. Panel (c) further shows that depletion-driven changes in signal variability are also anti-correlated with changes in standard deviation.

To further assess whether the effects of dopamine depletion are specific to SE or SD, or both, we repeated the PLS analysis using the SD of the BOLD time series before and after dopamine depletion. The analysis revealed no significant effects of dopamine depletion on SD (permuted $p = 0.38$). We then regressed out SD from SE in each region for each participant and condition using a linear regression model and repeated the PLS analysis on the SD-residualized SE values. No statistically significant differences were detected using the SD-residualized SE values (permuted $p = 0.9$), indicating that SD and SE are not wholly independent of each other. Altogether the results suggest that SD and SE are both sensitive to the variance of the signal, but that SE captures additional temporal irregularities, making it more likely to detect the effects of dopamine depletion.

Discussion

We investigated the effect of dopamine depletion on the balance between local node properties and global network architecture. We report 2 key results: (1) dopamine depletion selectively destabilizes neural signaling, measured at the hemodynamic level, in salience and somatomotor networks, and (2) increased local variability in these intrinsic networks is accompanied by their disconnection from the global functional architecture. Altogether, these results point to a stabilizing influence of dopamine on neural signaling and highlight the link between local, node-level properties and global network architecture.

Linking Local and Global Dynamics

The present results highlight the relationship between local hemodynamic signal variability and functional embedding. Increased variability in salience and somatomotor networks was concomitant with decreased functional connectivity with the rest of the brain. It is possible that low dopamine states disrupt local neuronal signaling, making it less likely for remote populations to synchronize. Alternatively, dopamine depletion may disrupt inter-regional synchrony through a separate mechanism, resulting in greater local variability. The correlative nature of the results cannot be used to disambiguate these two possibilities and further causal experiments are necessary. The within-condition relationship between local variability and global connectivity remains an open question. In any case, the present report demonstrates that functional interactions span multiple topological scales, such that local and global dynamical properties cannot be fully appreciated in isolation (Cabral et al. 2011; Bolt et al. 2018).

Interestingly, dopamine depletion was associated with reduced between-module connectivity but not with within-module connectivity (Fig. 5). The effect was highly specific: reduced between-module connectivity was significantly observed only in networks that also experienced increased regional signal variability. In other words, dopamine depletion affected how nodes within these networks communicated with the rest of the brain, but did not affect their internal cohesion. A recent study demonstrated a similar effect at the level of resting state networks: networks with greater

temporal variability displayed greater within-network cohesion and lower between-network integration (Lee and Frangou 2017). Altogether, the present results highlight a simple principle: the tendency for nodes to form functional networks depends on their ability to synchronize with one another. Thus, functional interactions between regions must be studied together with the temporal properties of their local signals.

Recent theories emphasize dynamic over static brain function. At the network level, reconfiguration of functional interactions is increasingly recognized as an informative attribute of healthy brain function and dysfunction (Calhoun et al. 2014). Functional reconfiguration has been observed across multiple temporal scales, both at rest (Zalesky et al. 2014; Betzel et al. 2016) and with respect to a variety of cognitive functions (Shine et al. 2016a), including learning (Bassett et al. 2015; Mohr et al. 2016), attention (Shine et al. 2016b) and working memory (Kitzbichler et al. 2011), and even conscious awareness (Barttfeld et al. 2015; Godwin et al. 2015). In parallel, the dynamic range of local signal fluctuations has emerged as a node-level marker of brain function (Garrett et al. 2013a; Roberts et al. 2017). Traditionally disregarded as “noise”, changes in signal variability have been reported across the lifespan (McIntosh et al. 2008; Garrett et al. 2011; Guitart-Masip et al. 2015; Nomi et al. 2017), in multiple perceptual, cognitive and affective tasks (Mišić et al. 2010; Samanez-Larkin et al. 2010; Garrett et al. 2013b; Pfeiffer et al. 2018) and in a variety of psychiatric and neurological diseases (Mišić et al. 2015b; Bertrand et al. 2016; Mišić et al. 2016).

While most methods for estimating variability focus on node-level time series, several recent studies have conceptualized variability with respect to functional network embedding (Shen et al. 2015b; Mišić et al. 2016). For instance, local variability can be defined as the tendency for a node to switch network allegiance or to interact with multiple networks (Braun et al. 2015; Zhang et al. 2016). This dynamic network switching is conditioned by an underlying anatomy (Shen et al. 2015a; Zhang et al. 2016), but is also likely to be influenced by a variety of neurotransmitters. A prominent hypothesis is that dopamine modulates signal-to-noise ratio (Mohr and Nagel 2010; Samanez-Larkin et al. 2010). We turn to the specific role of dopamine next.

Dopamine and Signal Dynamics

Our results suggest that dopamine may act to stabilize neural signaling at the hemodynamic level, particularly in networks associated with motor control (somatomotor network) and orienting attention towards behaviorally-relevant stimuli (salience network). Dopamine depletion was simultaneously associated with increased within region signal variability and decreased extrinsic connectivity, indicating that dopaminergic signaling influences both local information processing and network-wide interactions. Importantly, the effects of depletion were not confined to a single locus but distributed over two large-scale networks, suggesting that even transient decreases in dopamine availability can disrupt local neuronal signaling and have far-reaching effects on synchrony among multiple systems.

There are two possible mechanisms by which dopamine depletion could cause the observed changes in cortical signal variability. The first possibility is that depletion modulates synaptic activity and signal gain directly via cortical receptors (Seamans and Yang 2004). Mechanistic studies *in vitro* have demonstrated that dopamine influences intrinsic ionic currents

and synaptic conductance (Durstewitz et al. 2000; Kroener et al. 2009). These modulatory effects may facilitate or suppress neural signaling, helping to stabilize neural representations. In addition, dose–response effects of dopamine release may be both tonic and phasic (Goto et al. 2007), with the two modes thought to be mediated by distinct signaling pathways and receptors, and manifesting in distinct behavioral outcomes (Cox et al. 2015). For instance, striatal medium spiny neurons of the direct pathway express D_1 receptors and are thought to promote movement and the selection of rewarding actions. Neurons in the indirect pathway mainly express D_2 receptors and are thought to inhibit cortical patterns that encode maladaptive or non-rewarding actions (Surmeier et al. 2011). Although our results are consistent with the broad notion that dopamine stabilizes neural representations to facilitate reward learning and movement, further experiments are necessary to determine whether the observed effects can be attributed to tonic or phasic modulation, and to D_1 or D_2 receptor transmission.

The second possibility is that the effects of dopamine depletion may originate in the striatum, an area with dense dopaminergic afferents as well as projections to both the somatomotor and salience networks (Alexander et al. 1986; Alexander and Crutcher 1990; Zhang et al. 2017). Prominent projections from dorsal striatum terminate in the somatomotor system (forming the motor loop), while projections ventral striatum terminate in the salience system. A dopaminergically-depleted striatum may therefore disrupt ongoing cortico-striatal signaling, resulting in downstream cortical effects, such as increased variability. Importantly, the two accounts are not mutually exclusive, and it is possible that the observed effects depend on both mechanisms.

Dopamine depletion can thus have local and global consequences, influencing a range of sensory-motor and higher cognitive functions. Age-related decline in dopaminergic transmission is hypothesized to lead to greater signal variability, influencing the distinctiveness of neural representations and, ultimately, performance (Mohr and Nagel 2010; Samanez-Larkin et al. 2010). The stabilizing role of dopamine can also be observed in diseases associated with dopaminergic dysfunction, such as Parkinson's disease (PD), attention deficit hyperactivity disorder (ADHD), and schizophrenia. In PD for instance, cell death in substantia nigra leads to reduced dopaminergic transmission, with extensive motor symptoms. Intriguingly, dopamine depletion in PD is associated with reduced cortico-striatal functional connectivity patterns and reduced gait automaticity (Gilat et al. 2017). Similarly, in ADHD, reduced dopamine signaling is associated with deficits in goal-directed behavior and reward learning (del Campo et al. 2013).

Finally, the present results draw attention to an overlooked assumption of graph-based models of brain structure and function: that all nodes are identical, except for their connectivity patterns. In other words, graph representations often ignore important inter-regional differences that could influence neural activity and synchrony, including morphology, cytoarchitectonics, gene expression, and receptor densities (Lariviere et al. 2018). How dopaminergic modulation interacts with modulation by other neurotransmitters is an exciting open question (Shine et al. 2018).

Measuring Signal Variability

Finally, we note that several recent reports have also investigated the role of dopaminergic signaling in the context of local

signal dynamics, but drew an altogether different conclusion: that dopamine up-regulation “increases” signal variance. Specifically, Alavash et al (2018) reported that L-dopa administration increased BOLD standard deviation during an auditory working memory task (a syllable pitch discrimination task). Similarly, Garrett and colleagues (2015) reported that *d*-amphetamine administration also increased signal standard deviation during a working memory task (a visual letter n-back task). Although we used a different method to manipulate dopamine (APTD vs. L-dopa and *d*-amphetamine) and to record hemodynamic activity (resting state vs. task), we believe that the primary difference between these studies and our own is how signal variability was operationalized. Namely, both Alavash et al. (2018) and Garrett et al. (2015) defined signal variability in terms of standard deviations. The results shown in Figure 1 and Figure S4 demonstrate that sample entropy and variance based measures (e.g., standard deviation) capture different aspects of signal variability. Most importantly, because of the way that sample entropy is used to detect repeating patterns in a signal, we find that in practice, the two measures are often anti-correlated, which explains the seemingly different results. Altogether, these studies demonstrate a need to further refine the concept of signal variability and for greater plurality of methods (Fulcher and Jones 2017). While some measures are sensitive to signal dispersion (e.g., standard deviation), others are sensitive to temporal regularity (e.g., sample entropy).

Methodological Considerations

Our results may depend on a number of methodological choices and potential limitations, which we consider in detail here. Methodological choices include the type of parcellation and resolution, intrinsic network definition, and parameter settings for SE. The reported effects are consistent across 5 resolutions (from 83 to 1015 nodes; Fig. S1), 3 network partitions (detected using clustering, Infomap, and Louvain methods; Fig. S3) and a range of parameter settings (Fig. S2). Although we took steps to mitigate concerns about these choices, the present results are based on a finite sampling of a multifactorial methodological space.

More generally, we studied the effects of dopamine depletion in the context of task-free, resting state fMRI, which presents 3 significant challenges for interpretation. First, dopaminergic transmission is inherently related to specific cognitive functions, which may be accessible without overt task demands. We find evidence that dopamine depletion affects information transfer in two intrinsic networks with specific functional properties, but more research is necessary to investigate how dopamine affects the function of these networks in the presence of task demands. Second, dopaminergic transmission within specific subcortical and cortical circuits occurs at time scales that may be inaccessible with BOLD imaging. The present results can be used to draw conclusions about slow, modulatory effects of dopamine, but more electrophysiological evidence is necessary to relate these effects to faster phasic dopaminergic responses. Third, the present data were collected during an eyes-open resting state scan, which may potentially entail different neurocognitive demands than eyes-closed, including recruitment of visuomotor and attention networks (Jao et al. 2013; Patriat et al. 2013).

Summary

Our results support a link between local node dynamics and network architecture. Pharmacological perturbation may

selectively target and disconnect specific networks without altering their internal cohesion. These results demonstrate that the effect of dopamine on synaptic signaling ultimately manifests at the level of large-scale brain networks.

Supplementary Material

Supplementary material is available at *Cerebral Cortex* online.

Authors' Contributions

Conceptualization, G.S., B.M., and A.D.; Methodology and Resources, C.A.C, J.T.C., A.N.-S., M.L., A.D.; Data Curation, Y.Z.; Formal Analysis and Investigation, G.S., Y.Z.; Writing-Original Draft, G.S., B.M., and A.D.; Writing-Review & Editing, G.S., Y.Z., M.L., B.M., and A.D.; Funding Acquisition, M.L., A.D., and B.M.

Notes

This research was undertaken thanks in part to funding from the Canada First Research Excellence Fund, awarded to McGill University for the Healthy Brains for Healthy Lives initiative. BM acknowledges support from the Natural Sciences and Engineering Research Council of Canada (NSERC Discovery Grant RGPIN #017-04 265) and from the Fonds de recherche du Québec – Santé (Chercheur Boursier). G.S. acknowledges support from the Healthy Brains for Healthy Lives (HBHL) initiative at McGill University. The authors gratefully acknowledge code from Dr. Richard F. Betzel (University of Pennsylvania, PA, USA) and Dr. Andrea Avena-Koenigsberger (Indiana University, IN, USA) to create the boxplot and scatter plot figures, respectively. *Conflict of Interest:* The authors declare no competing interests.

References

- Alavash M, Lim SJ, Thiel C, Sehm B, Deserno L, Obleser J. 2018. Dopaminergic modulation of hemodynamic signal variability and the functional connectome during cognitive performance. *Neuroimage*. 172:341–356.
- Alexander GE, Crutcher MD. 1990. Functional architecture of basal ganglia circuits: neural substrates of parallel processing. *Trends Neurosci*. 13(7):266–271.
- Alexander GE, DeLong MR, Strick PL. 1986. Parallel organization of functionally segregated circuits linking basal ganglia and cortex. *Annu Rev Neurosci*. 9(1):357–381.
- Avena-Koenigsberger A, Mišić B, Sporns O. 2018. Communication dynamics in complex brain networks. *Nat Rev Neurosci*. 19(1):17.
- Barttfeld P, Uhrig L, Sitt JD, Sigman M, Jarraya B, Dehaene S. 2015. Signature of consciousness in the dynamics of resting-state brain activity. *Proc Natl Acad Sci USA*. 112(3):887–892.
- Bassett DS, Porter MA, Wymbs NF, Grafton ST, Carlson JM, Mucha PJ. 2013. Robust detection of dynamic community structure in networks. *Chaos: An Interdisciplinary J Nonlinear Sci*. 23(1):013142.
- Bassett DS, Yang M, Wymbs NF, Grafton ST. 2015. Learning-induced autonomy of sensorimotor systems. *Nat Neurosci*. 18(5):744–751.
- Beharelle AR, Kovačević N, McIntosh AR, Levine B. 2012. Brain signal variability relates to stability of behavior after recovery from diffuse brain injury. *Neuroimage*. 60(2):1528–1537.
- Bellec P, Lavoie-Courchesne S, Dickinson P, Lerch JP, Zijdenbos AP, Evans AC. 2012. The pipeline system for Octave and Matlab (PSOM): a lightweight scripting framework and execution engine for scientific workflows. *Front Neuroinformatics*. 6:7.
- Bellec P, Rosa-Neto P, Lyttelton OC, Benali H, Evans AC. 2010. Multi-level bootstrap analysis of stable clusters in resting-state fMRI. *Neuroimage*. 51(3):1126–1139.
- Benjamini Y, Hochberg Y. 1995. Controlling the false discovery rate: a practical and powerful approach to multiple testing. *J Roy Stat Soc B*. 57(1):289–300.
- Bertrand J-A, McIntosh AR, Postuma RB, Kovacevic N, Latreille V, Panisset M, Chouinard S, Gagnon J-F. 2016. Brain connectivity alterations are associated with the development of dementia in Parkinson's disease. *Brain Conn*. 6(3):216–224.
- Betzel RF, Fukushima M, He Y, Zuo X-N, Sporns O. 2016. Dynamic fluctuations coincide with periods of high and low modularity in resting-state functional brain networks. *Neuroimage*. 127:287–297.
- Björklund A, Dunnett SB. 2007. Fifty years of dopamine research. *Trends Neurosci*. 30(5):185–187.
- Blondel VD, Guillaume J-L, Lambiotte R, Lefebvre E. 2008. Fast unfolding of communities in large networks. *J Stat Mech*. 2008(10):P10008.
- Bolt T, Prince EB, Nomi JS, Messinger D, Llabre MM, Uddin LQ. 2018. Combining region-and network-level brain-behavior relationships in a structural equation model. *Neuroimage*. 165:158–169.
- Braun U, Schäfer A, Walter H, Erk S, Romanczuk-Seiferth N, Haddad L, Schweiger JI, Grimm O, Heinz A, Tost H, et al. 2015. Dynamic reconfiguration of frontal brain networks during executive cognition in humans. *Proc Natl Acad Sci USA*. 112(37):11678–11683.
- Cabral J, Hugues E, Sporns O, Deco G. 2011. Role of local network oscillations in resting-state functional connectivity. *Neuroimage*. 57(1):130–139.
- Calhoun VD, Miller R, Pearlson G, Adalı T. 2014. The chronnectome: time-varying connectivity networks as the next frontier in fMRI data discovery. *Neuron*. 84(2):262–274.
- Cammoun L, Gigandet X, Meskaldji D, Thiran JP, Sporns O, Do KQ, Maeder P, Meuli R, Hagmann P. 2012. Mapping the human connectome at multiple scales with diffusion spectrum MRI. *J Neurosci Methods*. 203(2):386–397.
- Carbonell F, Nagano-Saito A, Leyton M, Cisek P, Benkelfat C, He Y, Dagher A. 2014. Dopamine precursor depletion impairs structure and efficiency of resting state brain functional networks. *Neuropharmacology*. 84:90–100.
- Costa M, Goldberger AL, Peng C-K. 2005. Multiscale entropy analysis of biological signals. *Phys Rev E*. 71:021906.
- Coull JT, Hwang HJ, Leyton M, Dagher A. 2012. Dopamine precursor depletion impairs timing in healthy volunteers by attenuating activity in putamen and supplementary motor area. *J Neurosci*. 32(47):16704–16715.
- Cox SM, Frank MJ, Larcher K, Fellows LK, Clark CA, Leyton M, Dagher A. 2015. Striatal d1 and d2 signaling differentially predict learning from positive and negative outcomes. *Neuroimage*. 109:95–101.
- Damoiseaux JS, Rombouts SA, Barkhof F, Scheltens P, Stam CJ, Smith SM, Beckmann CF. 2006. Consistent resting-state networks across healthy subjects. *Proc Natl Acad Sci*. 103(37):13848–13853.
- Deco G, Jirsa VK, McIntosh AR. 2010. Emerging concepts for the dynamical organization of resting-state activity in the brain. *Nat Rev Neurosci*. 12(1):nrn2961.
- del Campo N, Fryer TD, Hong YT, Smith R, Brichard L, Acosta-Cabrero J, Chamberlain SR, Tait R, Izquierdo D, Regenthal R, et al. 2013. A positron emission tomography study of nigro-

- striatal dopaminergic mechanisms underlying attention: implications for ADHD and its treatment. *Brain*. 136(11): 3252–3270.
- Desikan RS, Ségonne F, Fischl B, Quinn BT, Dickerson BC, Blacker D, Buckner RL, Dale AM, Maguire RP, Hyman BT, et al. 2006. An automated labeling system for subdividing the human cerebral cortex on MRI scans into gyral based regions of interest. *Neuroimage*. 31(3):968–980.
- Durstewitz D, Seamans JK, Sejnowski TJ. 2000. Dopamine-mediated stabilization of delay-period activity in a network model of prefrontal cortex. *J Neurophysiol*. 83(3): 1733–1750.
- Edgington E, Onghena P. 2007. Randomization tests. New York, NY: Chapman and Hall/CRC press.
- Efron B, Tibshirani R. 1986. Bootstrap methods for standard errors, confidence intervals, and other measures of statistical accuracy. *Statist Sci*. 1(1):54–75.
- Fulcher BD, Jones NS. 2017. hctsa: a computational framework for automated time-series phenotyping using massive feature extraction. *Cell Syst*. 5(5):527–531.
- Garrett DD, Kovacevic N, McIntosh AR, Grady CL. 2011. The importance of being variable. *J Neurosci*. 31(12):4496–4503.
- Garrett DD, McIntosh AR, Grady CL. 2013a. Brain signal variability is parametrically modifiable. *Cereb Cortex*. 24(11): 2931–2940.
- Garrett DD, Nagel IE, Preuschhof C, Burzynska AZ, Marchner J, Wiegert S, Jungehülsing GJ, Nyberg L, Villringer A, Li SC, et al. 2015. Amphetamine modulates brain signal variability and working memory in younger and older adults. *Proc Natl Acad Sci*. 112(24):7593–7598.
- Garrett DD, Samanez-Larkin GR, MacDonald SW, Lindenberger U, McIntosh AR, Grady CL. 2013b. Moment-to-moment brain signal variability: a next frontier in human brain mapping? *Neurosci Biobehav Rev*. 37(4):610–624.
- Gilat M, Bell PT, Martens KAE, Georgiades MJ, Hall JM, Walton CC, Lewis SJ, Shine JM. 2017. Dopamine depletion impairs gait automaticity by altering cortico-striatal and cerebellar processing in Parkinson's disease. *Neuroimage*. 152: 207–220.
- Godwin D, Barry RL, Marois R. 2015. Breakdown of the brain's functional network modularity with awareness. *Proc Natl Acad Sci USA*. 112(12):3799–3804.
- Gollo LL, Zalesky A, Hutchison RM, van den Heuvel M, Breakspear M. 2015. Dwelling quietly in the rich club: brain network determinants of slow cortical fluctuations. *Phil Trans R Soc B*. 370(1668):20140165.
- Goto Y, Otani S, Grace AA. 2007. The yin and yang of dopamine release: a new perspective. *Neuropharmacology*. 53(5): 583–587.
- Grandy TH, Garrett DD, Schmiedek F, Werkle-Bergner M. 2016. On the estimation of brain signal entropy from sparse neuroimaging data. *Scie Rep*. 6:23073.
- Guimerà R, Amaral LAN. 2005. Cartography of complex networks: modules and universal roles. *J Stat Mech*. 2005(02): P02001.
- Guitart-Masip M, Salami A, Garrett D, Rieckmann A, Lindenberger U, Bäckman L. 2015. Bold variability is related to dopaminergic neurotransmission and cognitive aging. *Cereb Cortex*. 26(5):2074–2083.
- Heisz JJ, Shedden JM, McIntosh AR. 2012. Relating brain signal variability to knowledge representation. *Neuroimage*. 63(3): 1384–1392.
- Jao T, Vértes PE, Alexander-Bloch AF, Tang IN, Yu YC, Chen JH, Bullmore ET. 2013. Volitional eyes opening perturbs brain dynamics and functional connectivity regardless of light input. *Neuroimage*. 69:21–34.
- Kitzbichler MG, Henson RN, Smith ML, Nathan PJ, Bullmore ET. 2011. Cognitive effort drives workspace configuration of human brain functional networks. *J Neurosci*. 31(22): 8259–8270.
- Krishnan A, Williams LJ, McIntosh AR, Abdi H. 2011. Partial Least Squares (PLS) methods for neuroimaging: a tutorial and review. *Neuroimage*. 56(2):455–475.
- Kroener S, Chandler LJ, Phillips PE, Seamans JK. 2009. Dopamine modulates persistent synaptic activity and enhances the signal-to-noise ratio in the prefrontal cortex. *PLoS One*. 4(8):e6507.
- Lariviere S, Vos de Wael R, Paquola C, Hong SJ, Mišić B, Bernasconi N, Bernasconi A, Bonilha L, Bernhardt B. 2018. Microstructure-informed connectomics: enriching large-scale descriptions of healthy and diseased brains. *Brain Connect*. <https://doi.org/10.1089/brain.2018.0587> Just Accepted.
- Le Masurier M, Zetterström T, Cowen P, Sharp T. 2014. Tyrosine-free amino acid mixtures reduce physiologically-evoked release of dopamine in a selective and activity-dependent manner. *J Psychopharmacol*. 28(6):561–569.
- Lee WH, Frangou S. 2017. Linking functional connectivity and dynamic properties of resting-state networks. *Sci Rep*. 7(1): 16610.
- Leyton M, Dagher A, Boileau I, Casey K, Baker GB, Diksic M, Gunn R, Young SN, Benkelfat C. 2004. Decreasing amphetamine-induced dopamine release by acute phenylalanine/tyrosine depletion: a PET/[11C] raclopride study in healthy men. *Neuropsychopharmacology*. 29(2):427.
- Leyton M, Young SN, Pihl RO, Etezadi S, Lauze C, Blier P, Baker GB, Benkelfat C. 2000. Effects on mood of acute phenylalanine/tyrosine depletion in healthy women. *Neuropsychopharmacology*. 22(1):52–63.
- McAuley J. 2003. The physiological basis of clinical deficits in Parkinson's disease. *Prog Neurobiol*. 69(1):27–48.
- McIntosh AR, Kovacevic N, Itier RJ. 2008. Increased brain signal variability accompanies lower behavioral variability in development. *PLoS Comput Biol*. 4(7):e1000106.
- McIntosh AR, Lobaugh NJ. 2004. Partial least squares analysis of neuroimaging data: applications and advances. *Neuroimage*. 23:S250–S263.
- McIntosh AR, Mišić B. 2013. Multivariate statistical analyses for neuroimaging data. *Annu Rev Psychol*. 64(1):499–525.
- McTavish SF, Cowen PJ, Sharp T. 1999a. Effect of a tyrosine-free amino acid mixture on regional brain catecholamine synthesis and release. *Psychopharmacology (Berl)*. 141(2):182–188.
- McTavish SF, McPherson MH, Sharp T, Cowen PJ. 1999b. Attenuation of some subjective effects of amphetamine following tyrosine depletion. *J Psychopharmacol*. 13(2): 144–147.
- Mišić B, Betzel RF, Nematzadeh A, Goñi J, Griffa A, Hagmann P, Flammini A, Ahn Y-Y, Sporns O. 2015a. Cooperative and competitive spreading dynamics on the human connectome. *Neuron*. 86(6):1518–1529.
- Mišić B, Doesburg SM, Fatima Z, Vidal J, Vakorin VA, Taylor MJ, McIntosh AR. 2015b. Coordinated information generation and mental flexibility: large-scale network disruption in children with autism. *Cereb Cortex*. 25(9): 2815–2827.
- Mišić B, Dunkley BT, Sedge PA, Da Costa L, Fatima Z, Berman MG, Doesburg SM, McIntosh AR, Grodecki R, Jetly R, et al. 2016. Post-traumatic stress constrains the dynamic repertoire of neural activity. *J Neurosci*. 36(2):419–431.

- Mišić B, Mills T, Taylor MJ, McIntosh AR. 2010. Brain noise is task dependent and region specific. *J Neurophysiol.* 104(5):2667–2676.
- Mišić B, Vakorin VA, Paus T, McIntosh AR. 2011. Functional embedding predicts the variability of neural activity. *Front Syst Neurosci.* 5:90.
- Mohr PN, Nagel IE. 2010. Variability in brain activity as an individual difference measure in neuroscience? *J Neurosci.* 30(23):7755–7757.
- Mohr H, Wolfensteller U, Betzel RF, Mišić B, Sporns O, Richiardi J, Ruge H. 2016. Integration and segregation of large-scale brain networks during short-term task automatization. *Nat Commun.* 7:13217.
- Montgomery AJ, McTavish SF, Cowen PJ, Grasby PM. 2003. Reduction of brain dopamine concentration with dietary tyrosine plus phenylalanine depletion: an [¹¹C] raclopride pet study. *Am J Psychiatry.* 160(10):1887–1889.
- Nagano-Saito A, Cisek P, Perna AS, Shirdel FZ, Benkelfat C, Leyton M, Dagher A. 2012. From anticipation to action, the role of dopamine in perceptual decision making: an fMRI-tyrosine depletion study. *J Neurophysiol.* 108(2):501–512.
- Nagano-Saito A, Leyton M, Monchi O, Goldberg YK, He Y, Dagher A. 2008. Dopamine depletion impairs frontostriatal functional connectivity during a set-shifting task. *J Neurosci.* 28(14):3697–3706.
- Newman MEJ, Girvan M. 2004. Finding and evaluating community structure in networks. *Phys Rev E.* 69:026113.
- Nomi JS, Bolt TS, Ezie CC, Uddin LQ, Heller AS. 2017. Moment-to-moment BOLD signal variability reflects regional changes in neural flexibility across the lifespan. *J Neurosci.* 37(22):5539–5548.
- Palmour RM, Ervin FR, Baker GB, Young SN. 1998. An amino acid mixture deficient in phenylalanine and tyrosine reduces cerebrospinal fluid catecholamine metabolites and alcohol consumption in vervet monkeys. *Psychopharmacology (Berl).* 136(1):1–7.
- Patriat R, Molloy EK, Meier TB, Kirk GR, Nair VA, Meyerand ME, Prabhakaran V, Birn RM. 2013. The effect of resting condition on resting-state fMRI reliability and consistency: a comparison between resting with eyes open, closed, and fixated. *Neuroimage.* 78:463–473.
- Pfeffer T, Avramiea AE, Nolte G, Engel AK, Linkenkaer-Hansen K, Donner TH. 2018. Catecholamines alter the intrinsic variability of cortical population activity and perception. *PLoS Biol.* 16(2):e2003453.
- Power JD, Barnes KA, Snyder AZ, Schlaggar BL, Petersen SE. 2012. Spurious but systematic correlations in functional connectivity MRI networks arise from subject motion. *Neuroimage.* 59(3):2142–2154.
- Power JD, Cohen AL, Nelson SM, Wig GS, Barnes KA, Church JA, Vogel AC, Laumann TO, Miezin FM, Schlaggar BL, et al. 2011. Functional network organization of the human brain. *Neuron.* 72(4):665–678.
- Ramdani C, Carbone L, Vidal F, Béranger C, Dagher A, Hasbroucq T. 2015. Dopamine precursors depletion impairs impulse control in healthy volunteers. *Psychopharmacology (Berl).* 232(2):477–487.
- Richman JS, Moorman JR. 2000. Physiological time-series analysis using approximate entropy and sample entropy. *Am J Physiol-Heart Circ Physiol.* 278(6):H2039–H2049.
- Roberts JA, Friston KJ, Breakspear M. 2017. Clinical applications of stochastic dynamic models of the brain, part II: A review. *Biol Psychiatry Cogn Neurosci Neuroimag.* 2(3):225–234.
- Rubinov M, Sporns O. 2010. Complex network measures of brain connectivity: uses and interpretations. *Neuroimage.* 52(3):1059–1069.
- Rubinov M, Sporns O. 2011. Weight-conserving characterization of complex functional brain networks. *Neuroimage.* 56(4):2068–2079.
- Rubinov M, Sporns O, van Leeuwen C, Breakspear M. 2009. Symbiotic relationship between brain structure and dynamics. *BMC Neurosci.* 10(1):55.
- Samanez-Larkin GR, Kuhnen CM, Yoo DJ, Knutson B. 2010. Variability in nucleus accumbens activity mediates age-related suboptimal financial risk taking. *J Neurosci.* 30(4):1426–1434.
- Schultz W. 2002. Getting formal with dopamine and reward. *Neuron.* 36(2):241–263.
- Seamans JK, Robbins TW. 2010. Dopamine modulation of the prefrontal cortex and cognitive function. The dopamine receptors. Totowa, NJ: Humana Press. p. 373–398.
- Seamans JK, Yang CR. 2004. The principal features and mechanisms of dopamine modulation in the prefrontal cortex. *Prog Neurobiol.* 74(1):1–58.
- Shen K, Hutchison RM, Bezgin G, Everling S, McIntosh AR. 2015a. Network structure shapes spontaneous functional connectivity dynamics. *J Neurosci.* 35(14):5579–5588.
- Shen K, Mišić B, Cipollini BN, Bezgin G, Buschkuhl M, Hutchison RM, Jaeggi SM, Kross E, Peltier SJ, Everling S, et al. 2015b. Stable longrange interhemispheric coordination is supported by direct anatomical projections. *Proc Natl Acad Sci USA.* 112(20):6473–6478.
- Shine JM, Bissett PG, Bell PT, Koyejo O, Balsters JH, Gorgolewski KJ, Moodie CA, Poldrack RA. 2016a. The dynamics of functional brain networks: integrated network states during cognitive task performance. *Neuron.* 92(2):544–554.
- Shine JM, Koyejo O, Poldrack RA. 2016b. Temporal metastates are associated with differential patterns of time-resolved connectivity, network topology, and attention. *Proc Natl Acad Sci USA.* 113(35):9888–9891.
- Shine JM, van den Brink RL, Hernaus D, Nieuwenhuis S, Poldrack RA. 2018. Catecholaminergic manipulation alters dynamic network topology across cognitive states. *Netw Neurosci.* 2(3):381–396.
- Small M, Tse C. 2004. Optimal embedding parameters: a modeling paradigm. *Physica D.* 194(3):283–296.
- Surmeier DJ, Carrillo-Reid L, Vargas J. 2011. Dopaminergic modulation of striatal neurons, circuits, and assemblies. *Neuroscience.* 198:3–18.
- Traud AL, Kelsic ED, Mucha PJ, Porter MA. 2011. Comparing community structure to characteristics in online collegiate social networks. *SIAM Rev.* 53(3):526–543.
- Yeo BTT, Krienen FM, Sepulcre J, Sabuncu MR, Lashkari D, Hollinshead M, Roffman JL, Smoller JW, Zöllei L, Polimeni JR, et al. 2011. The organization of the human cerebral cortex estimated by intrinsic functional connectivity. *J Neurophysiol.* 106(3):1125–1165.
- Zalesky A, Fornito A, Cocchi L, Gollo LL, Breakspear M. 2014. Time-resolved resting-state brain networks. *Proc Natl Acad Sci USA.* 111(28):10341–10346.
- Zhang J, Cheng W, Liu Z, Zhang K, Lei X, Yao Y, Becker B, Liu Y, Kendrick KM, Lu G, et al. 2016. Neural, electrophysiological and anatomical basis of brain-network variability and its characteristic changes in mental disorders. *Brain.* 139(8):2307–2321.
- Zhang Y, Larcher KMH, Mišić B, Dagher A. 2017. Anatomical and functional organization of the human substantia nigra and its connections. *eLife.* 6:e26653.